Analysis of Permeance vs. Support Porosity for Thin Film Composite Membranes

Ioannis H. Karampelas, Lingxiang Zhu, Weiguang Jia, Milad Yavari, Haiqing Lin and Edward P. Furlani
Department of Chemical and Biological Engineering, University at Buffalo, SUNY

ABSTRACT

Membranes are an important technology for industrial gas separation, seawater desalination and emerging applications such as CO_2 capture. The key in steady growth of membrane applications is high performance thin film composite (TFC) membranes comprised of a thin selective layer (~100 nm or less) on a porous support that provides mechanical strength. As the selective layer becomes thinner to increase gas permeance and thus reduce the capital cost, the support surface morphology restricts the concentration profile of the penetrant in the selective layer. This geometric restriction of membrane permeance has been demonstrated using computational simulations. However, there are no rigorous experimental results to verify the modeling results. In this presentation we compare the measured and predicted permeance for two-layer model TFC membranes that are respectively comprised of track-etched polycarbonate (PC), nanofiltration membranes and industrial polyethersulfone (PES) ultrafiltration membranes, as porous supports, and perfluorinated glassy polymers, Teflon AF1600 and Hyflon AD 80, with excellent film formation and good stability as the selective layer materials. We discuss the fabrication and characterization of the membranes and show that the measured membrane permeance is consistent with predictions obtained using a three-dimensional (3D) computational mass transport model that predicts the steady-state penetrant concentration in the selective layer.

Keywords: Thin film composite membranes, membrane permeance, support porosity, mass transport analysis

1. INTRODUCTION

Membrane technology has been widely used for gas separations, such as nitrogen enrichment from air, CO_2 removal from natural gas, and propylene/N_2 separation for propylene recovery from reactor purge streams, due to its inherent advantages such as low cost, high energy efficiency, simplicity and compactness [1]. The prevalence of membrane systems is due to their high selectivity, to achieve the purity required, and high permeance to achieve the separation with low membrane area requirements. Since the capital cost of the membrane systems often scales linearly with the membrane area, membranes with higher permeance are often pursued to reduce the cost and footprint, thus strengthening the competitive edge of membrane technology against conventional separation technologies such as distillation and absorption [2,3].

Thin film composite (TFC) membranes have been widely used for industrial gas separations. These are comprised of a thin selective layer (~100nm) that provides the molecular separation and a thick porous support layer (100 - 150μm) that provides mechanical strength with negligible resistance to gas flow [4-7]. A schematic of TFC membranes is shown in **Figs. 1a** and **1b** [3,7]. For an ideal TFC membrane, gas transport is controlled by the selective layer while the porous support has a negligible effect on gas permeation. An ideal TFC membrane can be characterized by gas permeance, P_A/l [8]:

$$\frac{P_A}{l} = \frac{N_A}{A_m\left(p_{2,A} - p_{1,A}\right)} \qquad (1)$$

where P_A (cm^3(STP) cm/cm^2 s cmHg) is the permeability coefficient of gas component A in the selective layer material independent of film thickness, l is the thickness of the selective layer (cm), N_A (cm^3(STP)/s) is the flux through the membrane, A_m is the membrane area (cm^2), and $p_{2,A}$ and $p_{1,A}$ are the partial pressure (cmHg) of component A in the feed and permeate, respectively. Since l cannot be directly measured for the TFC membranes, the membranes are often characterized using permeance (P_A /l) with a unit of gpu, where 1gpu = 10^{-6} cm^3(STP)/cm^2 s cmHg.

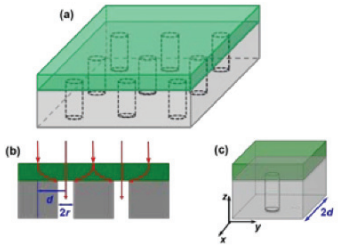

Figure 1. Schematic diagram illustrating (a) TFC membranes in three dimensional (3D) view; (b) a TFC membrane showing the geometric restriction by the pores with an average pore radius of r; and (c) a cubic unit cell used for the 3D computational simulation. $2d$: the length of a unit cell, porosity: $\phi = \pi r^2/4d^2$.

As shown in Eq. (1), one straightforward way to increase gas permeance is to decrease the thickness of the selective layer. However, as the selective layer thickness becomes comparable to the pore size of the porous support (10-50nm in radius), the available pores of the porous support may increase the effective diffusion path and influence the concentration gradient in the selective layer (as shown in **Fig. 1b**); both of which decrease the apparent gas permeance. The effect of the porous support structure on the gas permeance for component A can be characterized by membrane permeance efficiency (β_A), which is defined by [9,10]:

$$\beta_A = \frac{(P_A/l)_{Apparent}}{(P_A/l)_{Ideal}} \quad (2)$$

where $(P_A/l)_{Apparent}$ is the measured gas permeance for the TFC membrane, and $(P_A/l)_{Ideal}$ is the membrane permeance without the influence of the porous support (*i.e.*, $\phi = 1$). Lower β_A values indicate greater geometric restriction of the porous support on the gas permeation in the selective layer.

The geometric restriction of the molecule transport in the selective layer by the porous support has been recognized by Lonsdale and coworkers [9], who prepared composite membranes comprised of cellulose acetate thin films with various thicknesses on porous supports for desalination. The experimental results were also verified using a two-dimensional (2D) heat transfer model [9]. Rigorous 3D computational transport models with a unit cell as shown in **Fig. 1c** have been used to elucidate the impact of support structure on permeance [10-13]. These computational models provide a quantitative prediction of the penetrant concentration and diffusion streamlines, enabling an accurate prediction of the geometric restriction effect.

Despite advances in modeling the effect of porous support on gas permeances, there are no experimental results provided to directly validate the simulation results, presumably due to the challenges in the preparation of defect-free thin film composite membranes and accurate determination of the support morphology [14]. The typical porous supports (such as those made from polysulfone, polyacrylonitrile and polyimides) for the industrial thin film composite membranes do not have uniform pore size and porosity. Moreover, surface characterization techniques such as SEM may not provide an accurate description of the effective pore size and porosity in these supports because some pores on the surface may have dead-ends [15].

The objective of this study is to provide a rigorous understanding of the effect of the surface pore size and porosity of the porous support on gas permeance in the TFC membranes using an integrated experimental and simulation approach. Herein, track-etched polycarbonate (PC) nanofiltration membranes with uniform and straight pores, and polyethersulfone (PES) ultrafiltration membranes are used as model porous supports. The pore size and porosity are determined using the SEM and the dusty gas model (DGM). Thin film composite membranes were prepared using an amorphous perfluoropolymer (*i.e.*, Teflon® AF1600 and Hyflon® AD80) as the selective layer with varying thicknesses. The experimentally determined gas permeance is compared with the ideal permeance and simulated results obtained using a 3D mass transport modeling. The results are expected to provide a guideline for the design and selection of porous supports for TFC membranes.

2. COMPUTATIONAL MODEL

As shown in **Fig. 1b**, the geometric restriction enforced by the porous support leads to increased penetrant transport path length and uneven concentration gradient in the selective layer. A 3D computational mass transfer model provides an effective way to quantitatively describe streamlines, penetrant concentration gradient and flow rate in nanoscale structures [10-13,16-18]. In this work, a 3D model was developed for predicting the steady-state distribution of penetrant concentration and associated streamlines in the selective layer as a function key membrane parameters including the thickness of the selective layer and the porosity and pore size in the support layer. The model was implemented in a commercial program COMSOL Multiphysics® (www.comsol.com). The details are described in our previously published work [10] while key equation and assumptions are restated here to make our presentation more concise.

The steady-state concentration (C_A) of the penetrant in the selective layer is governed by the equation [10,11]:

$$\frac{\partial^2 C_A}{\partial x^2} + \frac{\partial^2 C_A}{\partial y^2} + \frac{\partial^2 C_A}{\partial z^2} = 0 \quad (3)$$

To simplify the analysis, the following assumptions are made: (a) the porous support contains a 2D ordered array of evenly-spaced cylindrical pores, as shown in **Fig. 1a**; (b) the lateral boundaries of the unit cell have symmetry-based zero flux in both the x and y directions (*i.e.*, perpendicular to the gas permeation direction); (c) the value of C_A is assumed to be 1 at the feed gas/selective layer interface and 0 at the selective layer/support pore interface; and (d) the solid fraction of the PC support is considered to be impermeable, since the gas permeability in the selective layer (Teflon AF1600) is about two orders of magnitude higher than that of polycarbonate. For example, the CO_2 permeability in Teflon AF1600 and PC is 520 Barrers [19] and 6.8 Barrers [20], respectively.

In these simulations, the porosity values of the porous supports were taken from the results of the dusty gas model. Since the simulated permeances depend on the the scaled selective layer thickness (S = *l/r*), instead of the absolute value of pore radii (*r*), the *r* value is set as 10nm for all the membranes, and the selective layer thickness is varied in the range between 5nm and 400nm to evaluate the effect of the scaled selective layer thickness on the membrane permeance efficiency (β_A).

3. EXPERIMETAL

Figure 2 summarizes the experimental procedures required to prepare and characterize TFC membranes. More details in preparation and characterization of TFC membranes, PC supports, PES supports, and intrinsic properties of Teflon AF1600 and Hyflon AD 80 are discussed in our published work [21,22].

4. RESULTS and DISCUSSION

To understand the geometric restriction of the porous support on gas permeance, the experimental data is compared to the CFD simulation results. **Figure 3a** compares the simulation with data from published literature including the 3D modeling analysis by Ramon and Hoek [19] and experimental data for water permeation by Lonsdale and coworkers [10]. Our simulation results are consistent with those performed by Ramon and Hoek for the porous support

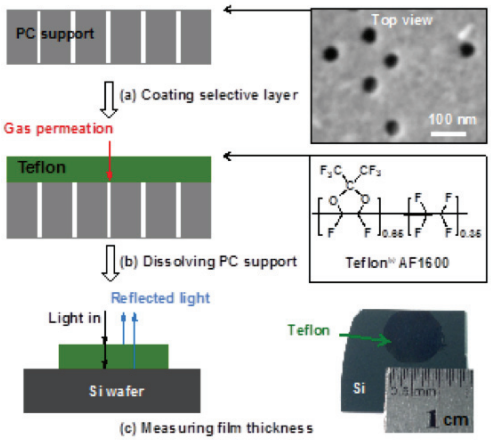

Figure 2. Experimental preparation and characterization thin film composite membranes, using Teflon AF1600/PC: (a) coating Teflon AF1600 thin film on the PC support such as PC-25 (with surface morphology shown on the right); (b) dissolving the PC support using chloroform after gas permeation measurement; and (c) determining the thin film thickness using a spectrometer and/or ellipsometer, after transferring to a silicon wafer.

with a porosity of 0.20 [47]. Moreover, our modeling can effectively describe the experimental data obtained by Lonsdale and coworkers except for the membranes with the scaled selective layer thicknesses ($S = l_s/r$) of 20-40, though the porous support used in their study had a porosity of 0.23, slightly higher than the value of 0.20 used in the simulation. The lower than expected water permeance may be caused by the pore penetration [9], which is not considered in our model.

Figure 3b shows the simulated membrane permeance efficiency for the membranes on the four PC supports as a function of the scaled selective layer thickness ($S = l_s/r$). Due to the low porosity ranging from 0.59% to 3.2% for the porous supports, the membranes show very low permeance efficiency, confirming the adverse effect of geometric restriction on gas permeance. The permeance efficiency decreases with a decreasing thickness of the selective layer, as the geometric restriction becomes more severe with the decrease in the scaled selective layer thickness. For example, for the PC-25 with a porosity of 3.2%, the permeance efficiency is 0.52 at an S value of 20, and it decreases to 0.21 when the S value decreases to 5. In general, the permeance efficiency appears to increase with increasing support porosity, *i.e.*, the order of permeance efficiency is the same as that of the porosity of the PC supports.

Figure 3b also directly compares the experimental results of the membranes with PC supports to the simulated results. The values of the experimental permeance efficiency are the average of those for four gases (*i.e.*, H_2, N_2, CH_4, and CO_2). The experimental results of the membranes with PC-50 and PC-25 are remarkably consistent to the simulated ones. On the other hand, the experimental results for the membranes on PC-15 and PC-7.5 are lower than the simulated ones. Presumably, this can be caused by pore penetration and/or uneven dispersion of pores on the support. The PC-25 and PC-50 have higher porosity and presumably would be less sensitive to such effects.

As shown in **Fig. 3c**, the experimental data for Teflon AF1600/PES and Hyflon AD80/PES TFC membranes are compared to the simulation results based on the effective surface porosity of 25% and 10%. The consistency is also remarkable, considering the complexity in charactering the support morphology and preparing defect-free ultrathin film membranes.

In conclusion, there is good consistency between the modeling and experiment results, validating that the support pore size and porosity enforces geometric restriction on the gas permeation in the TFC membranes, thus reducing gas permeance. When designing TFC membranes, supports with finer pores and higher porosity should be used. The pore dispersion of the supports also influences membrane permeance, hence, porous supports with uniform pore

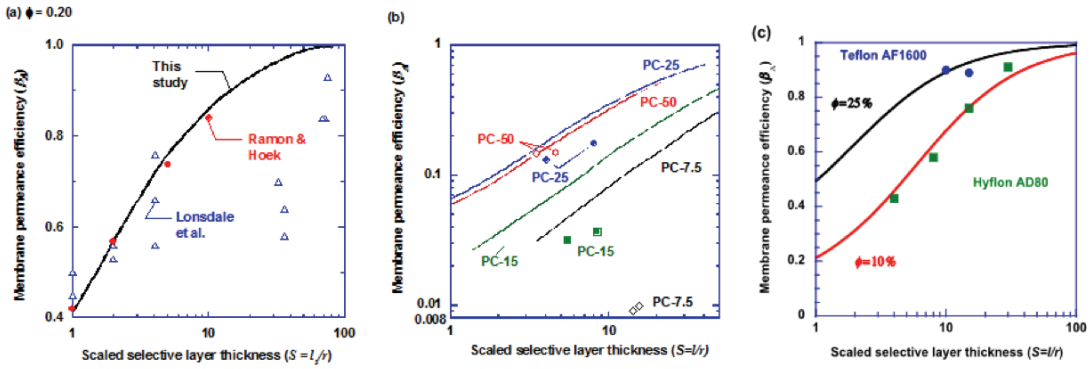

Figure 3. Effect of the support porosity and the scaled selective layer thickness on the membrane permeance efficiency. (a) Comparison of simulation results to published data; (b) comparison of modeling and experimental data for membranes with PC supports. The porosity of the PC supports follows the order: PC-25 (3.2%) > PC-50 (2.8%) > PC-15 (1.1%) > PC-7.5 (0.59%). (c) Geometric restriction of PES porous support on gas permeance: comparison of experimental membrane permeance efficiency (solid dots) to modeling results.

dispersion are preferred.

5. CONCLUSIONS

This study convincingly verifies that the porosity, pore size and pore dispersion of the porous support exerts geometric restrictions on the gas transport in the thin selective layer, resulting in the decrease in the gas permeance of the thin film composite membranes. There is good agreement between the experimental and CFD simulation data, confirming that porous supports pose significant geometric restrictions on gas permeation. The restriction becomes more severe with decreasing support porosity and scaled selective layer thickness. Both experimental and simulation results based on the model supports suggest that high flux TFC membranes require supports with high porosity and small pores with regular arrangement.

ACKNOWLEDGEMENTS

We gratefully acknowledge the financial support of the Korean Carbon Capture and Sequestration R&D Center and the New York State Center of Excellence in Materials Informatics at University at Buffalo. We also like to thank Dr. Hans Wijmans at Membrane Technology and Research, Inc. for his comments and suggestions.

REFERENCES

[1] D. E. Sanders, Z. P. Smith, R. L. Guo, L. M. Robeson, J. E. McGrath, D. R. Paul, and B. D. Freeman, Energy-efficient polymeric gas separation membranes for a sustainable future: A review, Polymer, 54 (2013) 4729-4761.

[2] H. Lin, Integrated membrane material and process development for gas separation, Curr. Opin. Chem. Eng., 4 (2014) 54-61.

[3] H. Lin*, et al.*, Membrane-based oxygen-enriched combustion, Ind. Eng. Chem. Res., 52 (2013) 10820-10834.

[4] I. Cabasso and K. A. Lundy, Method of making memranes for gas separation and the composite membranes, US Patent 4602922, 1986.

[5] K. A. Lundy and I. Cabasso, Analysis and construction of multilayer composite membranes for the separation of gas mixtures, Ind. Eng. Chem. Res., 28 (1989) 742-756.

[6] J. Shieh, T. Chung, and D. R. Paul, Study on multi-layer composite hollow fiber membranes for gas separation, Chem. Eng. Sci., 54 (1999) 675-684.

[7] R. W. Baker and B. Low, Gas separation membrane materials: A perspective, Macromolecules, 47 (2014) 6999-7013.

[8] J. G. Wijmans and R. W. Baker, The solution-diffusion model: A review, J. Membr. Sci., 107 (1995) 1-21.

[9] H. K. Lonsdale, R. L. Riley, C. R. Lyons, and D. P. Carosella, Transport in composite reverse osmosis membranes, in M. Bier (Ed.), Membrane processes in industry and biomedicine, Plenum Press, New York, 1971, pp. 101-122.

[10] M. Kattula, K. Ponnuru, L. Zhu, W. Jia, H. Lin, and E. P. Furlani, Designing ultrathin film composite membranes: The impact of gutter layer, Sci. Rep., 5, DOI: 10.1038/srep15016 (2015).

[11] G. Z. Ramon, M. C. Y. Wong, and E. M. V. Hoek, Transport through composite membrane, part 1: Is there an optimal support membrane?, J. Membr. Sci., 415 (2012) 298-305.

[12] G. Z. Ramon and E. M. V. Hoek, Transport through composite membranes, part 2: Impacts of roughness on permeability and fouling, J. Membr. Sci., 425 (2013) 141-148.

[13] J. G. Wijmans and P. J. Hao, Influence of the porous support on diffusion in composite membranes, J. Membr. Sci., 494 (2015) 78-85.

[14] I. Cabasso, K. Robert, E. Klein, and J. Smith, Porosity and pore size determination in polysulfone hollow fibers, J. Appl. Polym. Sci., 21 (1977) 1883-1900.

[15] A. M. Davis and C. R. Ethier, Transport through materials bounded by porous surfaces, Chem. Eng. Sci., 49 (1993) 1655-1663.

[16] S. A. Khashan, A. Alazzam, and E. P. Furlani, Computational analysis of enhanced magnetic bioseparation in microfluidic systems with flow-invasive magnetic elements, Sci. Rep., 4 (2014).

[17] R. Ghidossi, D. Veyret, and P. Moulin, Computational fluid dynamics applied to membranes: State of the art and opportunities, Che. Eng. Proc., 45 (2006) 437-454.

[18] S. X. Liu, M. Peng, and L. M. Vane, Cfd simulation of effect of baffle on mass transfer in a slit-type pervaporation module, J. Membr. Sci., 265 (2005) 124-136.

[19] T. C. Merkel, I. Pinnau, R. S. Prabhakar, and B. D. Freeman, Gas and vapor transport properties of perfluoropolymers, in B. D. Freeman, Y. P. Yampolskii and I. Pinnau (Eds.), Materials science of membranes for gas and vapor separation, Wiley, 2006, pp. 251-270.

[20] W. J. Koros, A. H. Chan, and D. R. Paul, Sorption and transport of various gases in polycarbonate, J. Membr. Sci., 2 (1977) 165-190.

[21] L. Zhu, W. Jia, M. Kattula, K. Ponnuru, E. P. Furlani, and H. Lin, Effect of porous supports on the permeance of thin film composite membranes: Part i. Track-etched polycarbonate supports, J. Membr. Sci. (2016) In press, DOI:10.1016/j.memsci.2015.11.043

[22] L. Zhu, M. Yavari, W. Jia, E. P. Furlani, and H. Lin, Effect of porous supports on permeances of thin film composite membranes: Part ii. Industrial polyethersulfone supports, J. Membr. Sci., (2016) submitted.